IEEE Access
Multidisciplinary | Rapid Review | Open Access Journal

Received 20 August 2023, accepted 2 September 2023, date of publication 5 September 2023, date of current version 26 September 2023.

Digital Object Identifier 10.1109/ACCESS.2023.3312328

RESEARCH ARTICLE

FMCW Radar-Based Human Sitting Posture Detection

GUOXIANG LIU, XINGGUANG LI, CHUNSHENG XU, LEI MA, AND HONGYE LI
Changchun University of Science and Technology, Changchun, Jilin 130012, China
Corresponding author: Xingguang Li (Leexingguang@126.com)

ABSTRACT Sitting posture is closely related to our health. Poor sitting posture can cause various diseases and harm our physical health. Current methods to detect sitting posture include machine vision, wearable sensors, and pressure sensors. However, these methods have problems with respect to privacy, inconvenience, and cost. In this work, we proposed the use of frequency-modulated continuous wave radar (FMCW) for detecting human sitting posture, which employs wireless signal transmission to enable non-contact detection, protect privacy, and reduce costs. First, the range fast Fourier transform (FFT) and Doppler FFT of the radar's intermediate frequency (IF) signals are performed to obtain range and Doppler feature information for different sitting postures. Second, to overcome the problem of range FFT bin offset, a single target angle measurement method is proposed to obtain angle features. Subsequently, we constructed various combinations of features to explore the influence of different combinations of features on the detection of posture while sitting. And we used five machine learning algorithms to perform sitting posture detection experiments. Finally, we conducted sedentary experiments in an office setting and provided sitting history records. The experimental results demonstrate that the method we proposed can identify five distinct sitting postures with an average accuracy of 98.07%.

INDEX TERMS Frequency modulated continuous wave radar, sitting posture detection, machine learning.

I. INTRODUCTION

In today's society, people are increasingly spending their time sitting in their free time and at work [1]. According to statistics, 54.9% of people's waking hours are spent on sedentary behavior [2]. Unfortunately, this sedentary lifestyle has been associated with various health problems, such as diabetes [3], metabolic syndrome [4], cardiovascular disease [5], musculoskeletal symptoms [6], and obesity in adolescents [7], [8], [9]. Poor posture can further compromise the body by affecting spine stability [10], increasing hip pressure [11], and ultimately increasing the risk of low back pain [12], [13], [14], neck and back pain [15], [16], [17], [18], [19], [20]. In fact, low back pain and neck pain are the highest healthcare expenditures of 154 conditions in the United States in 2016, estimated at $1,345 billion [21]. Therefore, it is essential to detect sitting posture and remind people to sit properly to reduce the risk of these conditions and decrease healthcare care expenditure. Maintaining a correct sitting posture is essential for healthy living.

Currently, three main methods are used to detect sitting posture: wearable sensor-based, machine vision-based, and pressure sensor-based. The sensor-based method of the wearable [22], [23], [24], [25], [26] is usually expensive, difficult to install, and uncomfortable to wear, resulting in poor user experience. On the other hand, the pressure sensor-based method [27], [28], [29], [30], [31], [32] typically requires more sensors for accurate detection of sitting and can be costly. The machine vision-based method [33], [34], [35], [36], [37] is capable of accurately identifying different sitting postures, but is affected by the intensity of light and poses a risk of privacy leakage during the detection process.

In recent years, frequency-modulated continuous wave (FMCW) radar has become a popular sensor for human activity recognition due to its non-contact nature, high accuracy, independence from light and ability to protect user privacy [38]. Researchers have used FMCW radar to recognize various human activities and fall detection, Saeed et al. [39]

The associate editor coordinating the review of this manuscript and approving it for publication was Seifedine Kadry.

fused time Doppler features from multiple radars for recognition of human activities and fall detection. Ding et al. [40] extracted dynamic range-doppler trajectories of the human body from a series of range-doppler frames acquired by radar and used the residual network (ResNet) to identify five continuous human activities. Shrestha et al. [41] used continuous time series features of time range and time Doppler to identify six continuous human activities. Most of the features used by many researchers in human activity recognition are range or Doppler features. And recognized human activities belong mainly to a wide range of human activities. However, there may be some poor sitting postures with small changes in body amplitude (such as leaning to the left or right), which may not be obvious in range or Doppler features. Therefore, we considered whether new features can be introduced for the detection of posture while sitting.

Although FMCW radar has high angular resolution [38], Wang et al. [42] used a two-dimensional fast Fourier transform to construct time range and Doppler maps, and the music algorithm to construct time angle maps, and finally used dynamic time bending for gesture recognition. Wang et al. [43] utilized a dual 3D convolutional neural network to extract the features of the Doppler range map and the range angle map for gesture recognition. Yang and Zheng [44] extracted the range, angle and Doppler trajectory features of gestures for gesture recognition using a reused long-short-term memory (LSTM) network. These studies have employed a wide range of features, including range, Doppler, and angle, for gesture recognition.

A. RELATED WORK

In this section, we review the related work on human sitting posture detection (in Table 1) and discuss their methods and results.

Cajamarca et al. [26] placed three accelerometers in the upper body, middle body, and lower body of the elderly to detect eight types of physical activity, achieving an accuracy of 93.5% using decision trees. Jiang et al. [25] used an intelligent vest with a self-powered sensor to recognize six sitting postures of the human using a random forest with an accuracy of 96.6%. Although methods using wearable sensors can detect some posture during sitting, they also require users to wear related equipment at all times, which can result in poor user experience.

To increase the comfort and user experience of people, Pereira and Silva [27] fixed weight sensors in the chair and used KNN to classify seven postures of sitting, with a final precision of 87.5%. Hu et al. [30] designed a smart chair with six flexible sensors and other hardware, and used artificial neural network (ANN) classification to achieve an accuracy of 97.78% when recognizing seven sitting postures. Roh et al. [32] installed four force sensors on the chair seat plate and used SVM with radial basis function kernel to classify six sitting postures, achieving a maximum accuracy rate of 97.94%. Compared to methods using wearable sensors, sensor chairs can reduce user discomfort but have poorly portable and require reinstallation of sensors when changing chairs.

Cai et al. [29] used a seat cushion consisting of pressure sensors for the detection of sitting posture, and achieved an accuracy of 95.67% in the detection of six sitting postures using the improved self-organizing map-based sitting posture recognition (ISOM-SPR) method. Bourahmoune et al. [28] used the life chair lot cushion, which consists of pressure sensors, and achieved an accuracy of over 97.94% in recognizing six sitting postures with a stretch. Ran et al. [31] collected seven sitting postures using pressure sensors and achieved a precision of 97.07% using a five-layer artificial neural network. The use of seat cushions with built-in pressure sensors can increase portability and provide good recognition performance, but these performances are provided by the number of sensors used and may not be suitable for universal use.

Min et al. [33] used the Microsoft Kinect sensor to detect and track key skeletal points of the human body, and then used the faster region-based convolutional neural network (Faster R-CNN) to extract features and recognize nine postures of human sitting with an accuracy of 95.6%. Lan et al. [35] used the Hausdorff method to detect the position and size of the face and then recognized the postures of human sitting by comparing real-time contour features with standard contour features. However, the detection accuracy may decrease in the presence of poor lighting conditions. Using machine vision methods with fewer sensors, high portability, and no need for constant wear can achieve high detection accuracy, but the process requires continuous image acquisition and is sensitive to light intensity. In addition, since photos of people can be collected during this process, there may be a risk of privacy leakage.

The methods employed by the aforementioned research scholars for human sitting detection mainly involve wearable sensors, pressure sensors, and visual sensors. The use of wearable sensors allows for some sitting detection, but also requires the user to wear the device at all times, resulting in a poor experience. The use of pressure sensors is often costly due to the number of sensors used. Visual sensors are vulnerable to light, possess a low recognition rate under low light conditions, and pose a privacy risk. In contrast, this work proposes the use of the FMCW radar for the detection of human sitting.

B. CONTRIBUTION

In this work, we tried to use multiple range, Doppler, and angle features for human sitting detection by FMCW radar. First, protects privacy, while the FMCW allows for non-contact human sitting detection, providing a comfortable experience for the user; we demonstrate that only one FMCW radar is used for sitting posture detection, increasing portability while reducing hardware complexity and cost of use. The contributions of this work are as follows.

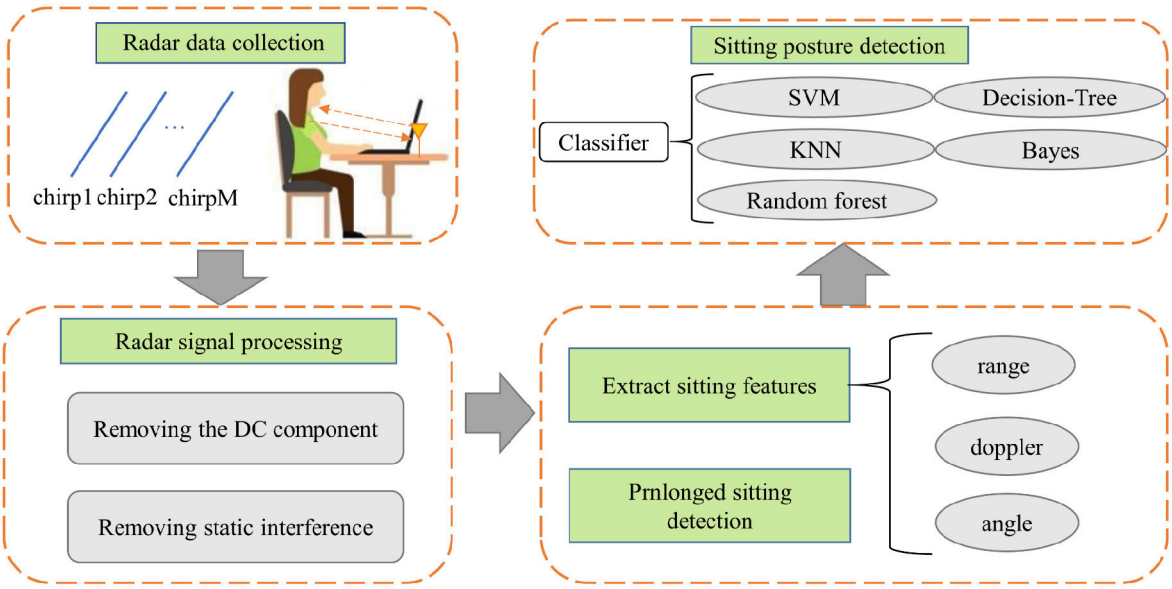

FIGURE 1. Based on FMCW radar sitting posture detection system.

TABLE 1. Comparison of different methods of detecting sitting posture.

Reference	Sensor type	Posture number	Classification method	Accuracy
[25]	Self-powered sensor	6	Random Forest	96.6%
[26]	Accelerometer	8	Decision Tree	93.5%
[27]	Load cell	7	KNN	87.5%
[28]	Pressure sensing	6	Random Forest	97.94%
[29]	Pressure sensing	6	ISOM	95.67%
[30]	Flex sensor	7	ANN	97.78%
[31]	Pressure sensing	7	Artificial Neural Network	97.07%
[32]	Pressure sensing	6	SVM	97.94%
[33]	Kinect	8	Faster R-CNN	95.6%

First, this work proposes the use of FMCW radar for human sitting detection, which is more accurate and ensures privacy and security without the need for a wearable device. This is the first instance of the use of FMCW radar technology for the detection of sitting posture in humans.

Second, this work proposes a method to calculate the angle of a single target to avoid angle measurement errors caused by range-fast Fourier transform (FFT) bin shifts during actual measurement. This method obtains angle information from the target without determining the target position.

Third, this work conducted experiments in the office to analyze and test the performance of different feature combination methods. And using five machine learning methods for sitting posture detection. Finally, the range-angle feature combination was selected for sitting posture detection. And the average accuracy of the five sitting postures detection is 98.07% by using support vector machines (SVM).

The structure of the paper is as follows. In Part II we present the methodological principles of FMCW radar sitting posture detection. In Part III, the experiments and results analysis are presented. Part IV compares and analyzes the methods proposed in this paper with recent posture detection methods. Finally, we present the conclusion of Part V.

II. METHOD

The FMCW radar sitting posture detection system in Fig.1. First, the FMCW radar acquires the sitting signal. Then preprocessed to remove the direct current (DC) component and surrounding static interference. Next, a feature extraction algorithm is used to extract the range, Doppler, and angle features of different sitting postures. And perform prolonged sitting detection. Finally, human sitting posture detection is performed. Further details of each component will be described later.

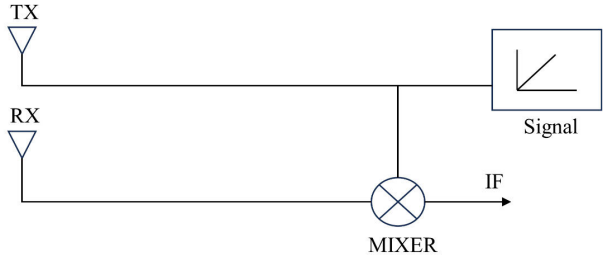

FIGURE 2. IF signal formation.

A. RADAR DATA COLLECTION

In this work, a sawtooth waveform was selected as the transmit waveform for the FMCW radar.

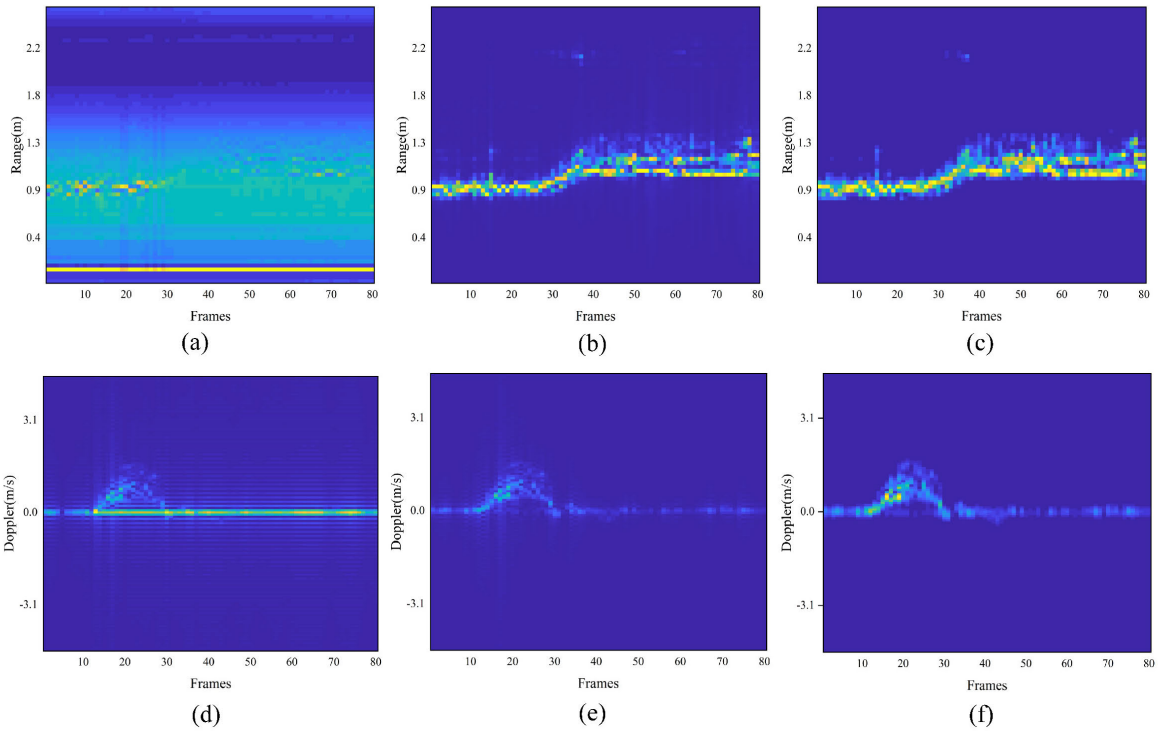

FIGURE 3. Signal processing results of the time-range map and the time-doppler map. (a), (d) Original. (b), (e) After DC removal. (c), (f) After applying the Hanning window.

According to [45], the transmit signal (Tx) in Fig. 2 of the FMCW radar is:

$$s_T(t) = A_T \cos\left(2\pi\left(f_c t + \frac{1}{2}\mu t^2\right) + \varphi_0\right) \tag{1}$$

where A_T represents the amplitude of the transmit signal, f_c denotes the carrier frequency, $\mu = B/T$ corresponds to the slope of the frequency, B signifies the bandwidth, T represents the duration of chirping, and φ_0 is the initial phase of the transmit signal. After the time delay of $t_l = 2 \times \frac{R_0+vt}{c}$, after phase shift $\Delta\varphi = \frac{4\pi f_c vt}{c}$,where R_0 is the distance at $t = 0$, v is the target velocity and c is the speed of light, the received echo signal can be expressed as:

$$s_R(t) = A_R \cos(2\pi(f_c(t - t_l) + \frac{1}{2}\mu(t - t_l)^2) + (\varphi_0 + \Delta\varphi)) \tag{2}$$

here A_R is the amplitude of the receiving signal. The transmit signal is mixed with the received signal by a mixer, and the IF signal is obtained by passing it through a low-pass filter:

$$s_{\mathrm{IF}}(t) = A_{\mathrm{IF}} \cos\left\{2\pi \cdot \mu\left(\frac{1}{2}t_l^2 - t_l t\right) - \Delta\varphi\right\} \tag{3}$$

here A_{IF} is the amplitude of the IF. Signals from different receiving antennas are combined to create a radar data cube (RDC) with dimensions of $(N * M * P)$, where N corresponds to the sampling points in each chirp, M represents the total number of chirps, and P denotes the quantity of the receiving antennas.

B. RADAR SIGNAL PROCESSING

Signal preprocessing is performed for each RDC. Specifically, the first is to subtract the average of frames from the frame value. This removes static interference [46] and the DC component from the data. Then, to reduce spectrum leakage, each RDC is multiplied by the Hanning window [43] as shown in Fig. 3. Next, the range FFT and doppler FFT are performed, and accumulation is carried out along the slow time dimension to obtain the time range map and the time-Doppler map in Fig. 3.

C. THE PROPOSED METHOD OF ANGLE ESTIMATION

In addition to the time-range map and time-Doppler map, it is also necessary to derive a time-angle map for various sitting postures. As depicted in Fig. 4, if the target is sufficiently distant from the radar, the incoming echo rays from the receiving antenna can be considered parallel to each other [45]. There exists an interval d between adjacent receiving antennas. And it varies in the actual echo distance is $dsin\theta$ and in time is $t = dsin\theta/v$. Consequently, the phase difference δ can be represented as follows.

$$\delta = \frac{2\pi d \sin\theta}{\lambda} \tag{4}$$

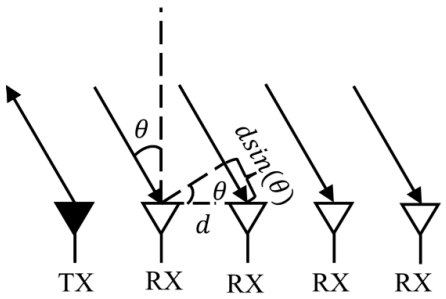

FIGURE 4. The methods for angle estimation.

where θ is the arrival angle, λ is the signal wavelength. The angle expression can be derived as follows:

$$\theta = sin^{-1}\left(\frac{\delta\lambda}{2\pi d}\right) \tag{5}$$

Previous studies usually require the determination of the target position in the Doppler range map to solve the angle of the target [43], [44], [47], [48]. If the target position determination is executed on the time range map [44], there will be range FFT bin shifts at various receiving antennas [49]. These shifts could lead to inaccuracies in the acquired phase. According to (5), there were errors in the resulting angle. To improve the precision of angle information and reduce the computational effort to determine the target position, we proposed an angle acquisition method that eliminates the effect of the FFT range bin offset [49] when dealing with a single target.

First, the IF signal is sampled to generate a discrete signal $s_{\mathrm{IF}}(n), n = 1, 2, \ldots N$, where N represents the sampling points. Next, the sampled IF signal undergoes the FFT:

$$S_{\mathrm{IF}}(k) = \sum_{n=0}^{N-1} s_{\mathrm{IF}}(n) e^{-j\frac{2\pi nk}{N}}; \quad k = 0 \ldots, N-1 \tag{6}$$

where the phase of the IF signal is $2\pi \cdot \mu\left(\frac{1}{2}t_l^2 - t_l k\right) - \Delta\varphi$,where $\Delta\varphi$ changes only after encountering the target. The phase corresponding to the N frequency points is then summed and averaged as follows:

$$\phi_p = \frac{1}{N}\sum_{K=1}^{N} 2\pi \cdot \mu\left(\frac{1}{2}t_l^2 - t_l k\right) - \frac{1}{N}\Delta\varphi_p \tag{7}$$

where N is the number of range FFT points, k is the range dimension sampling point, Therefore, the phase difference between adjacent received antenna signals can be expressed as:

$$\Delta\phi_p = \frac{1}{N}\left(\phi_p - \phi_{p-1}\right) \tag{8}$$

The target angle can be expressed as:

$$\theta = \sin^{-1}\left(\frac{\lambda\Delta\phi_p}{2\pi d}\right) \tag{9}$$

Algorithm 1 Feature Extraction

Input: time-range matrix M_{t-r},
time-velocity matrix M_{t-v},
time-angle matrix M_{t-a}, Averaging filter F_{ave}

Output: correct sitting feature $P_{cs}(rng, vel, ang)$, leaning Forward sitting feature $P_{lf}(rng, vel, ang)$, leaning backward $P_{lb}(rng, vel, ang)$, leaning left $P_{ll}(rng, vel, ang)$, leaning right $P_{lr}(rng, vel, ang)$

Compute the maximum amplitude M_{t-r}, denoted by N_{t-r};
Compute the maximum amplitude M_{t-v}, denoted by N_{t-v};
Compute the maximum amplitude M_{t-a}, denoted by N_{t-a};
$E_{t-r} = F_{ave}(N_{t-r})$;
$E_{t-v} = F_{ave}(N_{t-v})$;
$E_{t-a} = F_{ave}(N_{t-a})$;
Correct sitting: $P_{cs}(rng) = \max(E_{t-r})$;
$P_{cs}(vel) = \max(E_{t-v})$;
$P_{cs}(ang) = \max(E_{t-a})$;
Leaning forward: $P_{lf}(rng) = \max(E_{t-r})$;
$P_{lf}(vel) = \max(E_{t-v})$;
$P_{lf}(ang) = \max(E_{t-a})$;
Leaning backward: $P_{lb}(rng) = \max(E_{t-r})$;
$P_{lb}(vel) = \max(E_{t-v})$;
$P_{lb}(ang) = \max(E_{t-a})$;
Leaning left: $P_{ll}(rng) = \max(E_{t-r})$;
$P_{ll}(vel) = \max(E_{t-v})$;
$P_{ll}(ang) = \max(E_{t-a})$;
Leaning right: $P_{lr}(rng) = \max(E_{t-r})$;
$P_{lr}(vel) = \max(E_{t-v})$;
$P_{lr}(ang) = \max(E_{t-a})$;

D. MULTIPLE FEATURES EXTRACTION

Using effective features for various sitting postures is integral to classifying precision. Choosing too many irrelevant features not only increases computational complexity, but also negatively impacts classification performance. On the contrary, the selection of too few features could result in inaccurate classification, as the selected features may not entirely represent a certain sitting posture or lack defining characteristics. Therefore, to enhance feature selection, reduce the number of irrelevant attributes, and achieve improved classification accuracy, this work proposed a feature extraction method in Algorithm 1.

The first step is to select the point with the maximum energy in the feature map. Next, a mean filter [50] is applied for noise filtering in Fig. 5. Finally, the point with the largest absolute value is selected as the feature value of the target

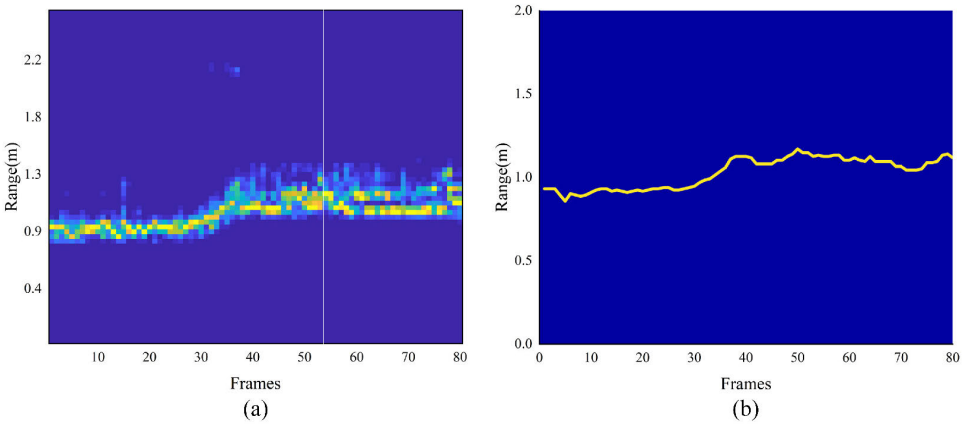

FIGURE 5. (a) The original of the time-range map. (b) Time-range map after extraction of maximum value and mean filtering.

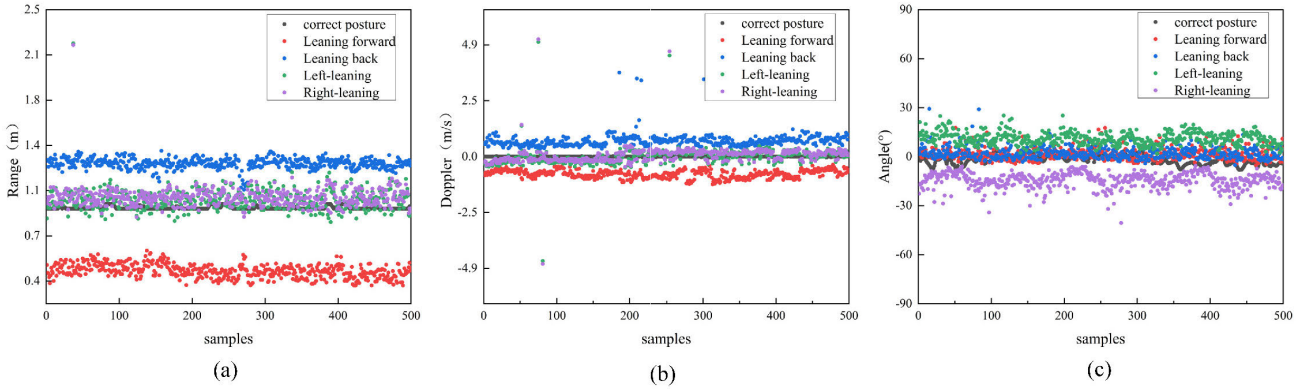

FIGURE 6. Different features of correct, leaning forward, leaning back, left-leaning, and right-leaning sitting postures. (a) Range features. (b) Doppler features. (c) Angle features.

sitting posture, shown in Fig. 6. From Fig. 6 (a) and Fig. 6 (b), we can see that the range and Doppler features can better distinguish between leaning forward and leaning backward, but it is difficult to distinguish between left-leaning, right-leaning and correct posture. From Fig. 6 (c), the angle feature can distinguish between left-leaning and right-leaning, but the features for leaning forward, leaning backward, and correct posture overlap. This shows that it is difficult to achieve sitting posture detection with a single feature.

Therefore, this work combined each feature of sitting posture to obtain four different feature combinations: range-angle, range-doppler, angle-doppler, and range-angle-doppler. In the fourth section, we analysed the performance of different combinations of features.

E. PROLONGED SITTING DETECTION

As shown in Fig. 7, when no one is sitting on the seat, the object detected by the radar is only the wall, with the target position approximately at 2 meters. When someone is sitting in a chair, the detected target changes into the human body. This is reflected in the time-range map. By setting a range threshold, we can detect whether there is someone sitting in the seat and then perform posture detection. For more detailed implementation, please refer to Algorithm 2.

F. DETECTION OF SITTING POSTURE

Machine learning techniques have been extensively used for FMCW radar human activity recognition [40]. For example, Ding et al. [40] used the subspace the k-closest neighbor (KNN) subspace to recognize continuous human activity. Similarly, Erol et al. [51] used a fusion of two classifiers, KNN and SVM, for the detection of human falls, and Amin et al. [52] employed the Gaussian kernel SVM for the detection of falls in the elderly. In this study, we experimented with different combinations of features using five distinct classifiers, namely SVM, KNN, Bayes, decision tree and random forest. Using 5-fold cross-validation to evaluate the detection results.

III. RESULT

A. EXPERIMENTAL EQUIPMENT AND EXPERIMENTAL DATA

This work employed the IWR6843ISK evaluation module and the DCA1000 evaluation module from Texas Instruments

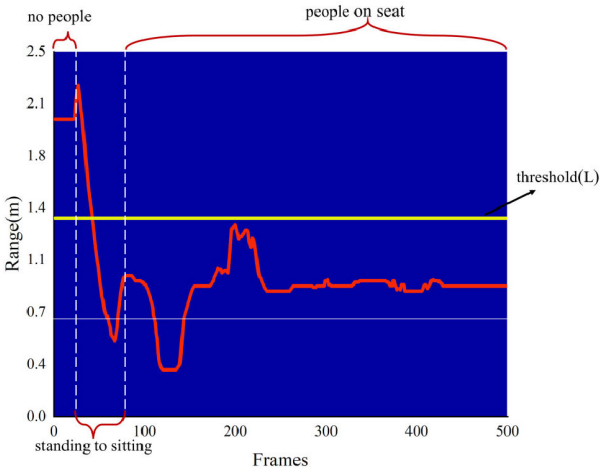

FIGURE 7. The principle of sedentary detection.

Algorithm 2 Prolonged Sitting Detection

Input: detection time T detection threshold L, sedentary time threshold t, Time-distance feature after mean filterinng E_{t-r}

Output: prolonged sitting-label

Initialize counter $a = 0$;
Initialize the frame $k = 1$;
for $k = 1{:}T$ **do**
  if $E_{t-r}(k) < L$ **then**
    $a = a + 1$;
    Perform sitting posture detection;
    if $a > t$ **then**
      prolonged sitting-label = 1;
      // judge as prolonged sitting;
      $a = 0$;
    end
  end
end

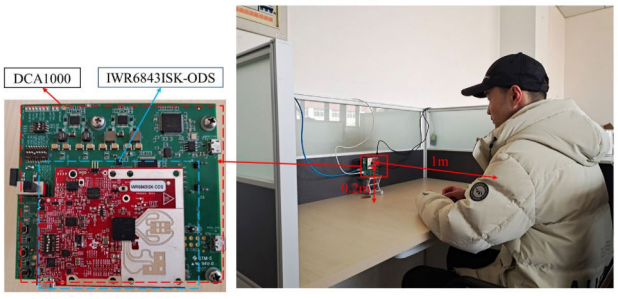

FIGURE 8. Used equipment and experimental scenario.

shown in Fig. 8. The system has an initial frequency of 60GHz, a maximum bandwidth of 4GHz, and three transmit and four receive antennas. A detailed parameter configuration is presented in Table 2.

TABLE 2. FMCW radar parameter configuration.

Parameter description	Value	Parameter description	Value
Bandwidth	3.6801GHz	ADC samples	64
Frequency slope	115.002MHZ /μs	Range resolution	0.0407m
Sample rate	2000ksps	Velocity resolution	0.0466m/s

FIGURE 9. Different perspectives of sitting postures. (a) Correct sitting posture. (b) Leaning forward. (c) Leaning back. (d) Left-leaning. (e) Right-leaning.

As shown in Fig. 8, in an office scenario, we installed the FMCW in the middle of the desk, facing toward the human body, with a distance of 1m, and the distance to the desktop is 0.2m. Then we selected five volunteers, including three men and two women. Each volunteer performed five different sitting postures as illustrated in Fig. 9 and recorded them, with each posture using the volunteer's most comfortable position. Each posture action lasted 80 frames, and we collected 500 pieces of information for each posture. In this way, it was able to obtain 2500 pieces of posture information. Randomly divided the data set into two groups, with 80% of the data in the training set and 20% of the data in the testing set.

B. CLASSIFIER PARAMETER CONFIGURATION

The classifier used comes from the sklearn library included in PyTorch. In this work, SVM was set with a linear kernel and a penalty parameter of 0.001. The multiclass form was set to One-vs-All (ova), the depth of the decision tree was set to 5, and K in KNN was set to 1.

C. THE PROPOSED SINGLE-TARGET ANGLE ACQUISITION METHOD

To demonstrate that the proposed single-target angle measurement method can reduce phase changes caused by range offset in this work. We tested with the left-leaning data.

In Fig.10, it can see that there are some deviations in phase extraction due to the range FFT offset when using the traditional method. The proposed method in this work can effectively reduce the phase deviation caused by the range offset and accurately detect the phase information of the target, thus obtaining the target angle.

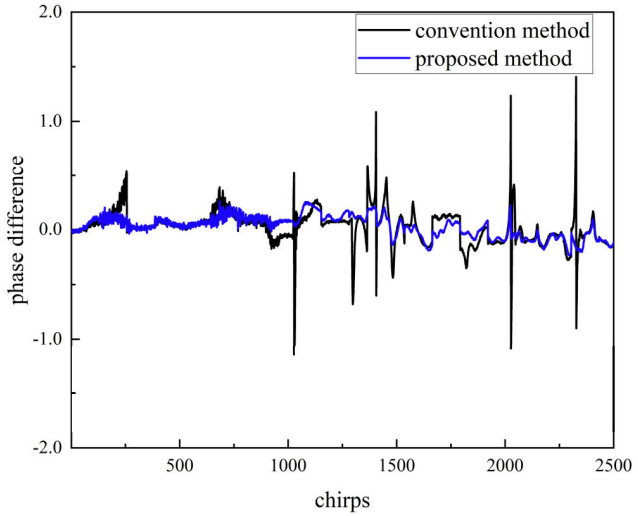

FIGURE 10. The phase difference obtained by the proposed method and the traditional methods.

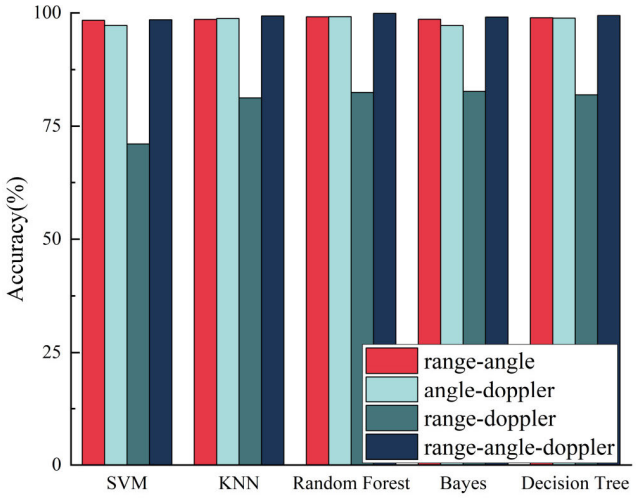

FIGURE 11. Accuracy of different combinations of features.

TABLE 3. FMCW radar parameter configuration.

	range-angle	angle-doppler	range-doppler	range-angle-doppler
SVM	98.36%	97.24%	71.04%	98.48%
KNN	98.56%	98.76%	81.24%	99.32%
Random Forest	99.13%	99.16%	82.48%	99.89%
Bayes	98.60%	97.20%	82.68%	99.08%
Decision Tree	98.92%	98.84%	81.92%	99.40%

D. DIFFERENT FEATURE COMBINATION PERFORMANCE ANALYSIS

The results of different feature combinations were discussed in this work. In Table 3, using the range-doppler feature combination, the SVM achieves an accuracy rate of 71.04%, KNN achieves 81.24%, random forest achieves 82.48%, Bayes achieves 82.68% and decision tree achieves 81.92%. The accuracies achieved by these five classifiers are lower than those achieved by using other combinations of features. However, the detection accuracy achieved using the combination of range angle, angle doppler, and range angle doppler features is relatively high in Fig. 11. These three combinations of features all include an angle feature, indicating that incorporating an angle feature into the detection of sitting posture is reasonable.

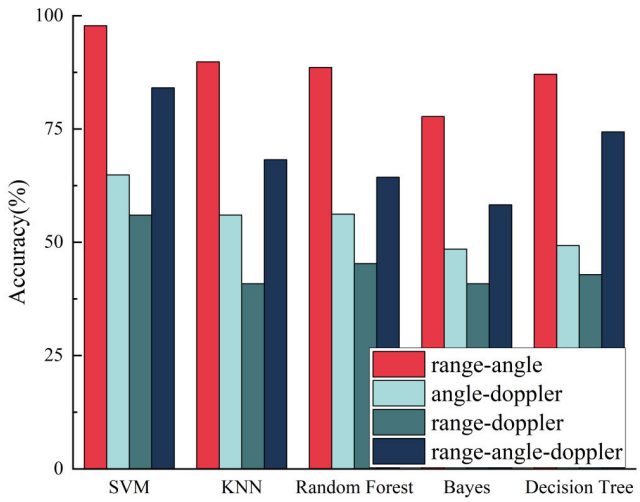

FIGURE 12. Accuracy of different combinations of features for the detection of continuous sitting posture.

TABLE 4. Accuracy of different feature combinations continuous sitting posture detection.

	range-angle	angle-doppler	range-doppler	range-angle-doppler
SVM	97.78%	64.86%	55.98%	84.07%
KNN	89.82%	56.00%	40.84%	68.20%
Random Forest	88.58%	56.18%	45.27%	64.34%
Bayes	77.73%	48.46%	40.84%	58.25%
Decision Tree	87.07%	49.27%	42.84%	74.36%

To further evaluate system performance, we simulate daily working conditions and randomly select three volunteers to collect short-term continuous posture data in an office environment. Each person collected 300 postures, resulting in a total of 900 posture data points. The detection results are shown in Fig. 12 and Table 4. As shown in Fig. 12 the accuracy using the range-Doppler feature combination is the lowest. The accuracy using the angle-doppler feature combination is better than that of the range-doppler feature combination, but worse than that of the range-angle-doppler feature combination. In Table 4, the accuracy using the

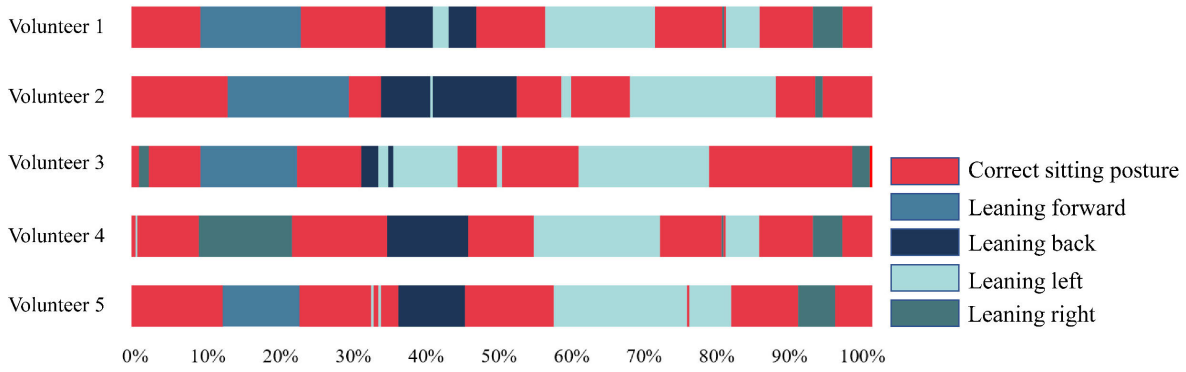

FIGURE 13. Observation of the sittingposture history.

combination of range angle features is the highest, achieving an accuracy rate of 97.78% by using SVM, 89.82% by using KNN, 85.58% by using random forest, 77.73% by using bayes, and 87.07% by using decision tree. Among these, the accuracy rate achieved by SVM is the highest at 97.78%. Taking into account the experimental results, the final choice for posture detection in sitting posture is the combination of range angle features with SVM classification in this work.

E. SEDENTARY BEHAVIOR HISTORY RECORDS

This work conducted a sedentary detection experiment with a detection time of 100 frames and a distance threshold of 1.4 m. Then we conducted 20 sets of 500-frame-long sedentary experiments. The detection results are shown in Table 5. The result of sedentary detection shows that the method we proposed is feasible.

TABLE 5. Results of sedentary detection.

Success	Failure
20	0

Additionally, this work had been provided with the historical posture records of five volunteers numbered 1 to 5, each consisting of 300 frames of sitting posture data in an office environment in Fig. 13.

In Fig.13, it can be observed that there are few misclassifications of posture between different posture switches for different individuals. This indicates that the system performance is relatively stable in this work. It also provides posture history records to assist doctors in diagnosis.

IV. CONCLUSION

In this work, we proposed a method for detecting human sitting posture based on FMCW radar. The method uses FMCW to detect changes in human sitting posture, extracts distance, angle, and Doppler features through a human sitting posture feature extraction algorithm, and then uses SVM to recognize 5 common human sitting posture states, achieving an average detection accuracy of 98.07%. At the same time, a single target human sitting posture recognition method is proposed to reduce phase error caused by distance FFT bin drift and improve target detection accuracy. Experimental results show that the method proposed in this article can effectively detect 5 postures of human sitting and provide a history of human sitting. Next, we will further expand the types of sitting postures and use deep learning for more complex posture detection.

REFERENCES

[1] C. E. Matthews, S. A. Carlson, and P. F. Saint-Maurice, "Sedentary behavior in U.S. adults: Fall 2019," *Med. Sci. Sports Exercise*, vol. 53, no. 12, pp. 2512–2519, Dec. 2021.

[2] C. E. Matthews, K. Y. Chen, and P. S. Freedson, "Amount of time spent in sedentary behaviors in the United States, 2003–2004," *Amer. J. Epidemiol.*, vol. 167, no. 7, pp. 875–881, Apr. 2008.

[3] J. G. van Uffelen, J. Wong, and J. Y. Chau, "Occupational sitting and health risks: A systematic review," *Amer. J. Preventive Med.*, vol. 39, no. 4, pp. 379–388, Oct. 2010.

[4] C. L. Edwardson, T. Gorely, M. J. Davies, L. J. Gray, K. Khunti, E. G. Wilmot, T. Yates, and S. J. H. Biddle, "Association of sedentary behaviour with metabolic syndrome: A meta-analysis," *PLoS ONE*, vol. 7, no. 4, Apr. 2012, Art. no. e34916.

[5] Z. T. Saleh, T. A. Lennie, and G. Mudd-Martin, "Decreasing sedentary behavior by 30 minutes per day reduces cardiovascular disease risk factors in rural Americans," *Heart Lung*, vol. 44, no. 5, pp. 382–386, Oct. 2015.

[6] P. Janwantanakul, P. Pensri, and V. Jiamjarasrangsri, "Prevalence of self-reported musculoskeletal symptoms among office workers," *Occupational Med.*, vol. 58, no. 6, pp. 436–468, Sep. 2008.

[7] J. Robatsch, P. Voitl, and S. C. Diesner-Treiber, "A cross-sectional, exploratory survey on health-relevant free-time activities and body mass index in preschool children in urban and rural settings of Austria," *BMC Pediatrics*, vol. 21, no. 1, p. 495, Nov. 2021.

[8] S. Dalibalta, A. Majdalawieh, S. Yousef, M. Gusbi, J. J. Wilson, M. A. Tully, and G. Davison, "Objectively quantified physical activity and sedentary behaviour in a young UAE population," *BMJ Open Sport Exercise Med.*, vol. 7, no. 1, Jan. 2021, Art. no. e000957.

[9] R. R. Pate, J. A. Mitchell, W. Byun, and M. Dowda, "Sedentary behaviour in youth," *Brit. J. Sports Med.*, vol. 45, no. 11, pp. 906–913, Sep. 2011.

[10] P. Waongenngarm, B. S. Rajaratnam, and P. Janwantanakul, "Internal oblique and transversus abdominis muscle fatigue induced by slumped sitting posture after 1 hour of sitting in office workers," *Saf. Health at Work*, vol. 7, no. 1, pp. 49–54, Mar. 2016.

[11] J.-S. Yu and D.-H. An, "Differences in lumbar and pelvic angles and gluteal pressure in different sitting postures," *J. Phys. Therapy Sci.*, vol. 27, no. 5, pp. 1333–1335, 2015.

[12] A. M. Lis, K. M. Black, H. Korn, and M. Nordin, "Association between sitting and occupational LBP," *Eur. Spine J.*, vol. 16, no. 2, pp. 283–298, Feb. 2007.

[13] P. Waongenngarm, B. S. Rajaratnam, and P. Janwantanakul, "Perceived body discomfort and trunk muscle activity in three prolonged sitting postures," *J. Phys. Therapy Sci.*, vol. 27, no. 7, pp. 2183–2187, 2015.

[14] K. T. Butte, D. Cannavan, J. Hossler, C. Travis, and J. Geiger, "The relationship between objectively measured sitting time, posture, and low back pain in sedentary employees during COVID-19," *Sport Sci. for Health*, vol. 19, no. 1, pp. 259–266, Mar. 2023.

[15] C.-C. Wu, C.-C. Chiu, and C.-Y. Yeh, "Development of wearable posture monitoring system for dynamic assessment of sitting posture," *Phys. Eng. Sci. Med.*, vol. 43, no. 1, pp. 187–203, Dec. 2019.

[16] J. P. Caneiro, P. O'Sullivan, A. Burnett, A. Barach, D. O'Neil, O. Tveit, and K. Olafsdottir, "The influence of different sitting postures on head/neck posture and muscle activity," *Manual Therapy*, vol. 15, no. 1, pp. 54–60, Feb. 2010.

[17] B. Zheng, L. Zheng, M. Li, J. Lin, Y. Zhu, L. Jin, R. You, Y. Gao, X. Liu, and S. Wang, "Sex differences in factors associated with neck pain among undergraduate healthcare students: A cross-sectional survey," *BMC Musculoskeletal Disorders*, vol. 23, no. 1, p. 842, Sep. 2022.

[18] P. B. O'Sullivan, A. J. Smith, D. J. Beales, and L. M. Straker, "Association of biopsychosocial factors with degree of slump in sitting posture and self-report of back pain in adolescents: A cross-sectional study," *Phys. Therapy*, vol. 91, no. 4, pp. 470–483, Apr. 2011.

[19] A. Syazwan, M. M. Azhar, and A. Anita, "Poor sitting posture and a heavy schoolbag as contributors to musculoskeletal pain in children: An ergonomic school education intervention program," *J. Pain Res.*, vol. 4, pp. 287–296, Sep. 2011.

[20] B. N. Da Rosa, T. S. Furlanetto, M. Noll, J. A. Sedrez, E. F. D. Schmit, and C. T. Candotti, "4-year longitudinal study of the assessment of body posture, back pain, postural and life habits of schoolchildren," *Motricidade*, vol. 13, no. 4, p. 3, Jan. 2018.

[21] J. L. Dieleman, J. Cao, and A. Chapin, "U.S. health care spending by payer and health condition, 1996–2016," *JAMA*, vol. 323, no. 9, pp. 863–884, Mar. 2020.

[22] C. Mattmann, O. Amft, and H. Harms, "Recognizing upper body postures using textile strain sensors," in *Proc. 11th IEEE Int. Symp. Wearable Comput.*, Oct. 2007, pp. 29–36.

[23] J. Estrada and L. Vea, "Real-time human sitting posture detection using mobile devices," in *Proc. IEEE Region 10 Symp. (TENSYMP)*, May 2016, pp. 140–144.

[24] L. Feng, Z. Li, C. Liu, X. Chen, X. Yin, and D. Fang, "SitR: Sitting posture recognition using RF signals," *IEEE Internet Things J.*, vol. 7, no. 12, pp. 11492–11504, Dec. 2020.

[25] Y. Jiang, J. An, F. Liang, G. Zuo, J. Yi, C. Ning, H. Zhang, K. Dong, and Z. L. Wang, "Knitted self-powered sensing textiles for machine learning-assisted sitting posture monitoring and correction," *Nano Res.*, vol. 15, no. 9, pp. 8389–8397, Sep. 2022.

[26] G. Cajamarca, I. Rodríguez, V. Herskovic, M. Campos, and J. Riofrío, "StraightenUp+: Monitoring of posture during daily activities for older persons using wearable sensors," *Sensors*, vol. 18, no. 10, p. 3409, Oct. 2018.

[27] L. Pereira and H. Plácido da Silva, "A novel smart chair system for posture classification and invisible ECG monitoring," *Sensors*, vol. 23, no. 2, p. 719, Jan. 2023.

[28] K. Bourahmoune, K. Ishac, and T. Amagasa, "Intelligent posture training: Machine-learning-powered human sitting posture recognition based on a pressure-sensing IoT cushion," *Sensors*, vol. 22, no. 14, p. 5337, Jul. 2022.

[29] W. Cai, D. Zhao, M. Zhang, Y. Xu, and Z. Li, "Improved self-organizing map-based unsupervised learning algorithm for sitting posture recognition system," *Sensors*, vol. 21, no. 18, p. 6246, Sep. 2021.

[30] Q. Hu, X. Tang, and W. Tang, "A smart chair sitting posture recognition system using flex sensors and FPGA implemented artificial neural network," *IEEE Sensors J.*, vol. 20, no. 14, pp. 8007–8016, Jul. 2020.

[31] X. Ran, C. Wang, Y. Xiao, X. Gao, Z. Zhu, and B. Chen, "A portable sitting posture monitoring system based on a pressure sensor array and machine learning," *Sens. Actuators A, Phys.*, vol. 331, Nov. 2021, Art. no. 112900.

[32] J. Roh, H.-J. Park, K. Lee, J. Hyeong, S. Kim, and B. Lee, "Sitting posture monitoring system based on a low-cost load cell using machine learning," *Sensors*, vol. 18, no. 2, p. 208, Jan. 2018.

[33] W. Min, H. Cui, Q. Han, and F. Zou, "A scene recognition and semantic analysis approach to unhealthy sitting posture detection during screen-reading," *Sensors*, vol. 18, no. 9, p. 3119, Sep. 2018.

[34] E. S. L. Ho, J. C. P. Chan, D. C. K. Chan, H. P. H. Shum, Y.-M. Cheung, and P. C. Yuen, "Improving posture classification accuracy for depth sensor-based human activity monitoring in smart environments," *Comput. Vis. Image Understand.*, vol. 148, pp. 97–110, Jul. 2016.

[35] M. Lan, L. Ke, and W. Chunhong, "A sitting posture surveillance system based on image processing technology," in *Proc. 2nd Int. Conf. Comput. Eng. Technol.*, 2010, pp. 692–695.

[36] B. Liu, Y. Li, S. Zhang, and X. Ye, "Healthy human sitting posture estimation in RGB-D scenes using object context," *Multimedia Tools Appl.*, vol. 76, no. 8, pp. 10721–10739, Apr. 2017.

[37] P. Paliyawan, C. Nukoolkit, and P. Mongkolnam, "Prolonged sitting detection for office workers syndrome prevention using Kinect," in *Proc. 11th Int. Conf. Elect. Eng./Electron., Comput., Telecommun. Inf. Technol. (ECTI-CON)*, 2014, pp. 1–6.

[38] H. Cui and N. Dahnoun, "High precision human detection and tracking using millimeter-wave radars," *IEEE Aerosp. Electron. Syst. Mag.*, vol. 36, no. 1, pp. 22–32, Jan. 2021.

[39] U. Saeed, S. Y. Shah, S. A. Shah, J. Ahmad, A. A. Alotaibi, T. Althobaiti, N. Ramzan, A. Alomainy, and Q. H. Abbasi, "Discrete human activity recognition and fall detection by combining FMCW RADAR data of heterogeneous environments for independent assistive living," *Electronics*, vol. 10, no. 18, p. 2237, Sep. 2021.

[40] C. Ding, H. Hong, Y. Zou, H. Chu, X. Zhu, F. Fioranelli, J. Le Kernec, and C. Li, "Continuous human motion recognition with a dynamic range-Doppler trajectory method based on FMCW radar," *IEEE Trans. Geosci. Remote Sens.*, vol. 57, no. 9, pp. 6821–6831, Sep. 2019.

[41] A. Shrestha, H. Li, J. Le Kernec, and F. Fioranelli, "Continuous human activity classification from FMCW radar with bi-LSTM networks," *IEEE Sensors J.*, vol. 20, no. 22, pp. 13607–13619, Nov. 2020.

[42] Y. Wang, A. Ren, M. Zhou, W. Wang, and X. Yang, "A novel detection and recognition method for continuous hand gesture using FMCW radar," *IEEE Access*, vol. 8, pp. 167264–167275, 2020.

[43] Y. Wang, D. Wang, Y. Fu, D. Yao, L. Xie, and M. Zhou, "Multi-hand gesture recognition using automotive FMCW radar sensor," *Remote Sens.*, vol. 14, no. 10, p. 2374, May 2022.

[44] Z. Yang and X. Zheng, "Hand gesture recognition based on trajectories features and computation-efficient reused LSTM network," *IEEE Sensors J.*, vol. 21, no. 15, pp. 16945–16960, Aug. 2021.

[45] W. Lei, L. Xu, X. Jiang, J. Luo, and F. Hou, "Automatic recognition of basic strokes based on FMCW radar system," *IEEE Sensors J.*, vol. 21, no. 13, pp. 15101–15113, Jul. 2021.

[46] S. Ahmed, W. Kim, J. Park, and S. H. Cho, "Radar-based air-writing gesture recognition using a novel multistream CNN approach," *IEEE Internet Things J.*, vol. 9, no. 23, pp. 23869–23880, Dec. 2022.

[47] P. Wang, J. Lin, F. Wang, J. Xiu, Y. Lin, N. Yan, and H. Xu, "A gesture air-writing tracking method that uses 24 GHz SIMO radar SoC," *IEEE Access*, vol. 8, pp. 152728–152741, 2020.

[48] Y.-C. Jhaung, Y.-M. Lin, C. Zha, J.-S. Leu, and M. Köppen, "Implementing a hand gesture recognition system based on range-Doppler map," *Sensors*, vol. 22, no. 11, p. 4260, Jun. 2022.

[49] K. Han and S. Hong, "Phase-extraction method with multiple frequencies of FMCW radar for human body motion tracking," *IEEE Microw. Wireless Compon. Lett.*, vol. 30, no. 9, pp. 927–930, Sep. 2020.

[50] H. Zhang, Y. Zhu, and H. Zheng, "NAMF: A nonlocal adaptive mean filter for removal of salt-and-pepper noise," *Math. Problems Eng.*, vol. 2021, Mar. 2021, Art. no. 4127679.

[51] B. Erol, M. Amin, and B. Boashash, "Range-Doppler radar sensor fusion for fall detection," in *Proc. IEEE Radar Conf. (RadarConf)*, May 2017, pp. 0819–0824.

[52] M. G. Amin, Y. D. Zhang, F. Ahmad, and K. C. D. Ho, "Radar signal processing for elderly fall detection: The future for in-home monitoring," *IEEE Signal Process. Mag.*, vol. 33, no. 2, pp. 71–80, Mar. 2016.

GUOXIANG LIU received the B.Eng. degree in electronic information engineering from the Changchun University of Science and Technology (CUST), Jilin, China, in 2020, where he is currently pursuing the M.S. degree in information and communication engineering. His research interests include radar signal processing, hand gesture recognition, sitting posture detection, and vital sign.

XINGGUANG LI received the M.S. and Ph.D. degrees in physical electronics from the Changchun University of Science and Technology (CUST), Jilin, China, in 2004 and 2010, respectively. He is currently a Professor with CUST. His research interests include radar signal processing and affective computing.

CHUNSHENG XU received the M.A.Eng. degree in electronic information engineering from the Changchun University of Science and Technology (CUST), Jilin, China, where he is currently pursuing the Ph.D. degree in information and communication engineering. His research interests include radar signal processing, human action recognition, and deep neural networks.

LEI MA received the B.Eng. degree in electronic information engineering from the Changchun University of Science and Technology (CUST), Jilin, China, in 2021, where he is currently pursuing the M.S. degree in information and communication engineering. His research interests include radar signal processing, human action recognition, and deep neural networks.

HONGYE LI received the B.Eng. degree in electronic information engineering from the Changchun University of Science and Technology (CUST), Jilin, China, in 2022, where he is currently pursuing the Ph.D. degree in information and communication engineering. His research interests include radar signal processing and hand gesture recognition.